Strained germanium thin film membrane on silicon substrate for optoelectronics

Donguk Nam,[1,*] Devanand Sukhdeo,[1] Arunanshu Roy,[1] Krishna Balram,[1] Szu-Lin Cheng,[2] Kevin Chih-Yao Huang,[1] Ze Yuan[1], Mark Brongersma,[3] Yoshio Nishi,[1] David Miller,[1] and Krishna Saraswat[1]

[1]*Department of Electrical Engineering, Stanford University, Stanford, California 94305, USA*
[2] *IBM T.J. Watson Research Center, 1101 Kitchawan Road, Yorktown Heights, New York 10598, USA*
[3]*Department of Materials Science and Engineering, Stanford University, Stanford, California 94305, USA*
[*]*dwnam@stanford.edu*

Abstract: This work presents a novel method to introduce a sustainable biaxial tensile strain larger than 1% in a thin Ge membrane using a stressor layer integrated on a Si substrate. Raman spectroscopy confirms 1.13% strain and photoluminescence shows a direct band gap reduction of 100meV with enhanced light emission efficiency. Simulation results predict that a combination of 1.1% strain and heavy n^+ doping reduces the required injected carrier density for population inversion by over a factor of 60. We also present the first highly strained Ge photodetector, showing an excellent responsivity well beyond 1.6um.

©2011 Optical Society of America

OCIS codes: (250.0250) Optoelectronics; (250.5960) Semiconductor lasers; (160.4670) Optical materials; (310.6860) Thin films, optical properties.

References and links

1. K. Koo, H. Cho, P. Kapur, and K. C. Saraswat, "Performance comparisons between carbon nanotubes, optical, and Cu for future high-performance on-chip interconnect applications," IEEE Trans. Electron. Dev. **54**(12), 3206–3215 (2007).
2. D. A. B. Miller, "Rationale and challenges for optical interconnects to electronic chips," Proc. IEEE **88**(6), 728–749 (2000).
3. D. J. Friedman, M. Meghelli, B. D. Parker, J. Yang, H. A. Ainspan, A. V. Rylyakov, Y. H. Kwark, M. B. Ritter, L. Shan, S. J. Zier, M. Sorna, and M. Soyuer, "SiGe BiCMOS integrated circuits for high-speed serial communication links," IBM J. Res. Develop. **47**(2), 259–282 (2003).
4. T. Krishnamohan, D. Kim, T. V. Dinh, A. T. Pham, B. Meinerzhagen, C. Jungemann, and K. C. Saraswat, "Comparison of (001), (110) and (111) Uniaxial- and Biaxial- Strained-Ge and Strained-Si PMOS DGFETs for All Channel orientations: Mobility Enhancement, Drive Current, Delay and Off-State Leakage", IEEE. IEDM. Tech. Digest., 899–892 (2008).
5. T.-H. Cheng, K.-L. Peng, C.-Y. Ko, C.-Y. Chen, H.-S. Lan, Y.-R. Wu, C. W. Liu, and H.-H. Tseng, "Strain-enhanced photoluminescence from Ge direct transition," Appl. Phys. Lett. **96**(21), 211108 (2010).
6. R. A. Soref and L. Friedman, "Direct-gap Ge/GeSn/Si and GeSn/Ge/Si heterostructures," Superlattices Microstruct. **14**(2–3), 189 (1993).
7. M. V. Fischetti and S. E. Laux, "Band structure, deformation potentials, and carrier mobility in strained Si, Ge, and SiGe alloys," J. Appl. Phys. **80**(4), 2234 (1996).
8. M. El Kurdi, G. Fishman, S. Sauvage, and P. Boucaud, "Band structure and optical gain of tensile-strained germanium based 30 band k·p formalism," J. Appl. Phys. **107**, 013710 (2010).
9. X. Sun, J. Liu, L. C. Kimerling, and J. Michel, "Room-temperature direct bandgap electroluminesence from Ge-on-Si light-emitting diodes," Opt. Lett. **34**(8), 1198–1200 (2009).
10. S. L. Cheng, J. Lu, G. Shambat, H. Y. Yu, K. Saraswat, J. Vuckovic, and Y. Nishi, "Room temperature 1.6 microm electroluminescence from Ge light emitting diode on Si substrate," Opt. Express **17**(12), 10019–10024 (2009).
11. P. H. Lim, S. Park, Y. Ishikawa, and K. Wada, "Enhanced direct bandgap emission in germanium by micromechanical strain engineering," Opt. Express **17**(18), 16358–16365 (2009).
12. M. El Kurdi, H. Bertin, E. Martincic, M. de Kersauson, G. Fishman, S. Sauvage, A. Bosseboeuf, and P. Boucaud, "Control of direct band gap emission of bulk germanium by mechanical tensile strain," Appl. Phys. Lett. **96**(4), 041909 (2010).
13. C. Boztug, F. Chen, J. Sanchez-Perez, F. Sudradjat, D. Paskiewicz, R.B. Jacobson, M. Lagally, and R. Paiella,

#154117 - $15.00 USD Received 7 Sep 2011; revised 12 Oct 2011; accepted 16 Oct 2011; published 5 Dec 2011

"Direct-bandgap germanium active layers pumped above transparency based on tensiley strained nanomembranes," CLEO:2011, PDPA2 (2011).
14. Y. Huo, H. Lin, Y. Rong, M. Makarova, M. Li, R. Chen, T. I. Kamins, J. Vuckovic, and J. S. Harris, "Efficient luminescence in highly tensile-strained germanium", IEEE Int. Conf. on Group IV Photonics, 265–267 (2009).
15. L. Nataraj, F. Xu, and S. G. Cloutier, "Direct-bandgap luminescence at room-temperature from highly-strained Germanium nanocrystals," Opt. Express **18**(7), 7085–7091 (2010).
16. J. R. Jain, D.-S. Ly-Gagnon, K. C. Balram, J. S. White, M. L. Brongersma, D. A. B. Miller, and R. T. Howe, "Tensile-strained germanium-on-insulator substrate fabrication for silicon-compatible optoelectronics", ArXiv preprint 1105.0044 (2011).
17. R. Soref, "Mid-infrared photonics in silicon and germanium," Nat. Photonics **4**(8), 495–497 (2010).
18. Y. Huo, R. Chen, H. Lin, T. I. Kamins, and J. S. Harris, "MBE growth of high Sn-percentage GeSn alloys with a composition-dependent absorption-edge shift," 7th Int. Conf. on Group IV Photonics Beijing, China (2010).
19. E. Kasper, M. Oehme, T. Aguirov, J. Werner, M. Kittler, and J. Schulze, "Room temperature direct band gap emission from Ge p-i-n heterojunction photodiodes", 7th Int. Conf. on Group IV Photonics Beijing, China (2010).
20. T. B. Boykin, N. Kharche, and G. Klimeck, "Brillouin-zone unfolding of perfect supercells having nonequivalent primitive cells illustrated with a Si/Ge tight-binding parameterization," Phys. Rev. B **76**(3), 035310 (2007).
21. T. B. Boykin, G. Klimeck, R. C. Bowen, and F. Oyafuso, "Diagonal parameter shifts due to nearest-neighbor displacements in empirical tight-binding theory," Phys. Rev. B **66**(12), 125207 (2002).
22. A. Nayfeh, C. O. Chui, T. Yonehara, and K. C. Saraswat, "Fabrication of high-quality p-MOSFET in Ge grown heteroepitaxially on Si," IEEE Electron Device Lett. **26**(5), 311–313 (2005).
23. Y. Ishikawa, K. Wada, J. Liu, D. D. Cannon, H.-C. Luan, J. Michel, and L. C. Kimerling, "Strain-induced enhancement of near-infrared absorption in Ge epitaxial layers grown on Si substrate," J. Appl. Phys. **98**(1), 013501 (2005).
24. J. T. L. Thong, W. K. Choi, and C. W. Chong, "TMAH etching of silicon and the interaction of etching parameters," Sens. Actuators A Phys. **63**(3), 243–249 (1997).
25. D. W. Hoffman and J. A. Thornton, "The compressive stress transition in Al, V, Zr, Nb and W metal films sputtered at low working pressures," Thin Solid Films **45**(2), 387–396 (1977).
26. Y. Bai, K. E. Lee, C. Cheng, M. L. Lee, and E. A. Fitzgerald, "Growth of highly tensile-strained Ge on relaxed $In_xGa_{1-x}As$ by metal-organic chemical vapor deposition," J. Appl. Phys. **104**(8), 084518 (2008).
27. J. Kim, S. W. Bedell, and D. K. Sadana, "Improved germanium n^+/p junction diodes formed by coimplantation of antimony and phosphorus," Appl. Phys. Lett. **98**(8), 082112 (2011).
28. G. Thareja, S. Chopra, B. Adams, Y. Kim, S. Moffatt, K. Saraswat, and Y. Nishi, "High n-type antimony dopant activation in germanium using laser annealing for n+/p junction diode," IEEE Electron Device Lett. **32**(7), 838–840 (2011).
29. Y. Huo, H. Lin, R. Chen, M. Makarova, Y. Rong, M. Li, T. I. Kamins, J. Vuckovic, and J. S. Harris, "Strong enhancement of direct transition photoluminescence with highly tensile-strained Ge grown by molecular beam epitaxy," Appl. Phys. Lett. **98**(1), 011111 (2011).
30. G. F. Burkhard, E. T. Hoke, and M. D. McGehee, "Accounting for interference, scattering, and electrode absorption to make accurate internal quantum efficiency measurements in organic and other thin solar cells," Adv. Mater. (Deerfield Beach Fla.) **22**(30), 3293–3297 (2010).

1. Introduction

With the performance of on-chip copper wires rapidly reaching its limit due to continuous scaling, optical interconnects are becoming the strongest candidate to replace electrical interconnects for low latency, high bandwidth and low power on-chip and off-chip communication [1,2]. In order to realize the integration of optical interconnects with silicon circuits, germanium (Ge) has recently gained an increasing amount of interest because of its complete compatibility with conventional CMOS processes [3]. Additionally, strain has been shown to increase the mobility in Ge channel MOSFETs [4].

Light emission in Ge is difficult to achieve because most of the injected electrons are pumped into the lower indirect L valley rather than the higher direct Γ valley resulting in a large fraction of non-radiative recombination [5]. However, since the difference between the Γ valley and the L valley in Ge is only 136meV and since approximately 1.7-1.9% in-plane biaxial tensile strain is known to transform Ge into the direct band gap material [6–8], research has increasingly focused on tensile strained Ge for efficient light emission. Recently, light emission by both optical and electrical pumping has been achieved from Ge grown on Si using a combination of tensile strain from a thermal expansion mismatch between Ge and Si and an indirect valley filling effect from heavy n-type doping [9,10]. Mechanically

#154117 - $15.00 USD Received 7 Sep 2011; revised 12 Oct 2011; accepted 16 Oct 2011; published 5 Dec 2011
(C) 2011 OSA

induced strain for further improvement in Ge light emission has also been researched. Modeling in Ref [11]. shows that Ge optical properties are expected to improve by micromechanical strain engineering using cantilever structures. Mechanically applying 0.37% biaxial strain on n-type Ge substrates has shown an enhancement of direct band gap recombination [5]. Recent work on relatively thick (28μm) membranes etched from bulk Ge has shown that tensile strain as large as 0.6% can be induced using a constant water pressure on the membrane [12]. Tensile strain as large as 2% in a very thin (20nm) Ge layer on a polymide film was temporarily achieved using high-pressure gas [13]. More than 2% tensile strain in Ge was demonstrated by growing a Ge layer on lattice relaxed InGaAs/GaAs buffer layers by molecular beam epitaxy (MBE) [14]. Other approaches include highly strained nanocrystal structures that show an increase by 2 orders of magnitude in photoluminescence as compared to bulk Ge [15]. Germainum-On-Insulator (GOI) substrate using layer transfer techniques presented 0.16% tensile strain for Ge optoelectronics [16]. GeSn is theoretically predicted to have a direct bandgap at an Sn concentration of 9% and the epitaxial growth of high-Sn concentration GeSn alloys is also experimentally demonstrated to show the bandgap reduction in the Γ valley [17,18]. Integration of both detectors and emitters on the same device structure using Ge grown by MBE has also recently been researched [19].

In this paper, we report a sustainable biaxial tensile strain larger than 1% using a thin (1.6μm) Ge membrane integrated on a Si substrate. Raman spectroscopy confirms the amount of tensile strain in membranes and photoluminescence shows a large enhancement in light emission efficiency as well as a direct bandgap reduction of nearly 100meV. Simulation results using a tight-binding model [20,21] predict that a combination of 1.1% tensile strain and $5x10^{19}cm^{-3}$ n-type doping can reduce the required injection carriers for population inversion in Ge by nearly two orders of magnitude compared to an undoped and unstrained Ge. In order to show the possibility of device integration, vertical PN photodetectors (PDs) are also fabricated on this highly strained membrane and photocurrent measurements show excellent responsivity well beyond 1.6μm in strained PDs. Our work opens up the possibility of easy fabrication for both optical and electronic devices integrated on a Si substrate.

2. Fabrication

A high quality n-type Ge membrane of 1.6μm thickness is fabricated using heteroepitaxial Ge growth on Si, in situ doping and a selective etching process as depicted in Fig. 1. First, a 500nm thick SiO_2 layer is thermally grown on a double-side polished Si wafer. Windows of various sizes are then defined by optical lithography on one side and the wafer is dipped into 6:1 buffered oxide etch (BOE) for 7 minutes to create an etch mask of patterned SiO_2. A 1.6μm thick n-type Ge layer is then grown on the bare Si side using multiple hydrogen annealing for heteroepitaxy (MHAH) for a high-quality and smooth-surface [22]. When the wafer cools down after the final hydrogen annealing at 825°C, 0.2% tensile strain is accumulated due to the large thermal expansion mismatch between n-type doped Ge and Si [23]. Then, approximately 205nm silicon nitride layer is deposited by plasma enhanced chemical vapor deposition (PECVD) as an anti-reflection coating in order to avoid Fabry-Perot modes in the thin Ge membrane. Using the patterned SiO_2 as an etch mask, Si is etched anisotropically from the back side in TMAH solution at 90°C for approximately 6 hours [24]. After Si is etched all the way up to the top Ge layer, a 1.6μm thick Ge membrane remains due to the high etch selectivity of Si over Ge in the TMAH solution. The membrane is still under 0.2% tensile strain since it is fixed at the edges and cannot relax. To further suppress Fabry-Perot modes, 80nm of titanium was deposited on the backside by a magnetron sputtering system, since the germanium has a lower reflection coefficient to titanium. Then, to introduce a higher tensile strain in this membrane, tungsten is deposited on the backside at 4mTorr pressure using a magnetron sputtering system. It is well known that the residual compressive stresses in tungsten can be larger than 4Gpa by lowering the chamber pressure [25]. As the

#154117 - $15.00 USD Received 7 Sep 2011; revised 12 Oct 2011; accepted 16 Oct 2011; published 5 Dec 2011
(C) 2011 OSA

compressive stressor tends to expand when it is released from a thick substrate, the membrane gets deflected and becomes tensile strained as shown in Fig. 1(b).

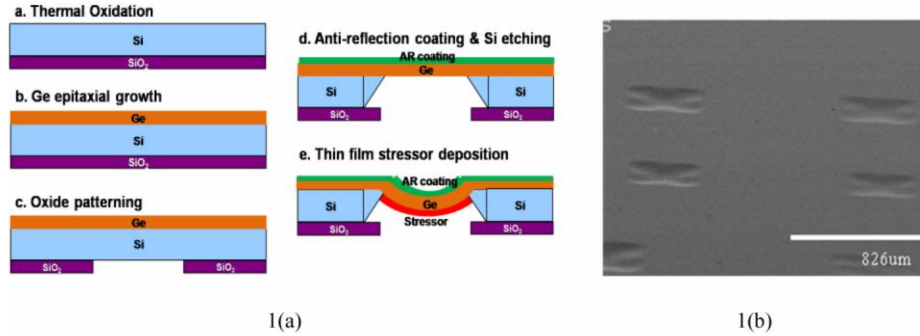

Fig. 1. (a) Fabrication process flow for highly strained Ge membrane (b) SEM picture of deflected membranes

3. Optical properties

A biaxial tensile strain larger than 1% was measured from both room temperature photoluminescence (PL) and Raman spectroscopy measurements. The excitation wavelengths were 532nm and 514nm for PL and Raman spectroscopy measurements, respectively. Both measurements were conducted at room temperature and the laser excitation power on the sample for PL was approximately 10mW. A strained InGaAs detector cooled to −100°C by liquid nitrogen was used to perform the measurements over an extended wavelength range.

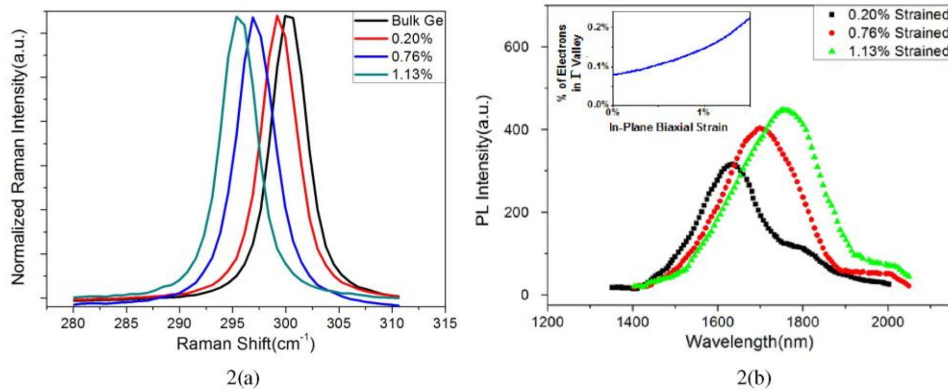

Fig. 2. (a) Normalized Raman spectra (b) Room temperature direct band gap PL spectra. The inset of the figure(b) shows how the percentage of electrons in the Γ valley increases with strain according to our simulations.

In Fig. 2(a), Raman spectroscopy measurements show the amount of bi-axial tensile strain in four different samples, crystalline Ge and Ge membranes with no stressor, 500nm, and 900nm tungsten stressor layers. Compared to crystalline Ge, the peak position shifts to the left as tensile strain is introduced in Ge membranes by thermal expansion mismatch for free standing membrane. The peak shifts even further by depositing thicker stressor layers. According to the equation for strain calculation from ref [26], the samples with 500nm and 900nm tungsten are under 0.76% ± 0.10% and 1.13% ± 0.13% biaxial tensile strain, respectively, where the errors are due to the resolution limit of the setup.

Photoluminescence measurements also confirmed a large tensile strain in our membrane as shown in Fig. 2(b). The dominant peaks are due to the transition from the direct Γ valley to the heavy-hole band [12,13]. Figure 2(b) shows the peak wavelengths of 1620nm, 1690nm

#154117 - $15.00 USD Received 7 Sep 2011; revised 12 Oct 2011; accepted 16 Oct 2011; published 5 Dec 2011
(C) 2011 OSA

and 1750nm for a free standing and strained membranes, respectively. Moreover, the integrated PL intensity from the 1.13% strained membrane is approximately twice as large as from the 0.2% strained membrane. The inset of Fig. 2(b) shows how the percentage of electrons in the Γ valley increases with strain, assuming heavy n-doping. This is because higher strain lowers the Γ valley edge relative to the L valley edge, thereby increasing spillover from the L valley into the Γ valley. Since the PL spectrum is dominated by transitions from the gamma valley, we expect the increase in gamma valley population to be roughly proportional to the integrated intensity of the PL signal. Comparing the 0.2% strained and 1.13% strained cases, our theoretical modeling of a 2x increase in Γ valley population is in good agreement with our experimental results which show approximately a 2x higher integrated PL intensity.

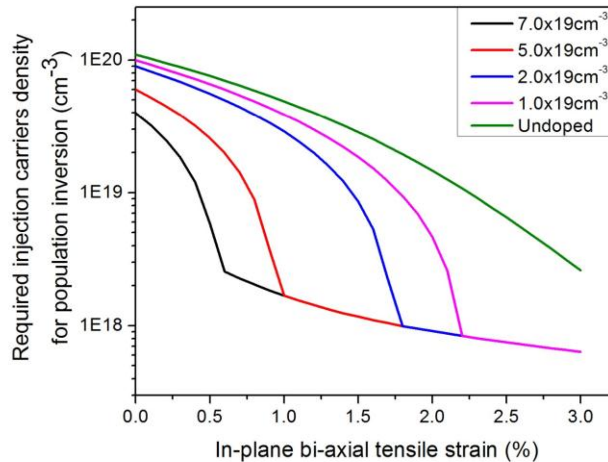

Fig. 3. Required injection carrier density for population inversion versus strain for different n-type doping concentration.

Looking toward future lasing applications, population inversion in Ge is much more readily achievable with a combination of n-doping, which begins filling the L-valley, and strain, which lowers the Γ-valley and also reduces the density of states in certain bands, notably the valence band. To quantify these changes, we have used sp3d5s* tight-binding with spin-orbital coupling [20], which incorporates diagonal parameter shifts due to the nearest-neighbor interactions when strain is present [21], to calculate the full band structure. From there, the carrier concentrations were approximated by summing the contributions from a mesh of evenly-spaced k-points over the entire first Brillouin zone. As shown in Fig. 3, our simulations predict that a combination of strain and n-doping would drastically reduce the amount of pumping required for population inversion (i.e. electron quasi-Fermi level within the gamma valley, and hole quasi-Fermi level within the valence band). While an undoped and unstrained Ge membrane would require pumping of $1.1 \times 10^{20} cm^{-3}$ to achieve population inversion, 1.1%-strained and $5 \times 10^{19} cm^{-3}$ n-doped Ge requires pumping of only $1.6 \times 10^{18} cm^{-3}$, a reduction of nearly two orders of magnitude. Note that the curves for n-doped Ge in Fig. 3 saturate to a lower bound with increased strain; this represents the region where the electron quasi-Fermi level is already near or above the Γ-valley, and so the required pumping is determined by how many carriers are needed to push the hole quasi-Fermi level down to the top of the valence band. Since n-type dopant activation in Ge higher than $5 \times 10^{19} cm^{-3}$ is readily achievable by either coimplantation of Sb and P [27] or laser annealing [28], our technique for larger than 1% strain strengthens the possibility of Ge laser for on-chip interconnects. It should also be noted that our simulations predict a crossover of the direct bandgap at roughly 2.2% strain, whereas most theoretical predictions claim the crossover

#154117 - $15.00 USD Received 7 Sep 2011; revised 12 Oct 2011; accepted 16 Oct 2011; published 5 Dec 2011
(C) 2011 OSA

occurs around 1.7-1.9% strain [6–8] and low-temperature PL experiments have suggested that 1.8% strain is already sufficient for a direct bandgap at 5K [29]. In addition, there is some error introduced by approximating the carrier density by summing over a finite number of k-points. However, increasing the density (and accuracy) of the mesh of k-points tends to return slightly lower carrier densities in all valleys, which would increase the enhancement from n-doping. Thus, our simulations are likely understating both the enhancement from strain and the enhancement from n-doping, and so these results should be viewed as pessimistic estimates.

4. Device realization

Vertical PN photodetectors (PDs) were fabricated on highly strained membranes to show the possibility of device integration using our technique. Figure 4(a) shows a schematic cross-section of a strained Ge PN photodetector. A 1.4μm undoped Ge and 250nm n^+-Ge layer is grown epitaxially using diluted 1% phosphine in situ doping without a subsequent annealing to avoid phosphorous dopant diffusion. A 450nm high Ge mesa is then patterned by dry etching, leaving p-type Ge as a supporting layer for a thin Ge membrane structure. Ti/Al metal contacts are realized by lift-off method for both n and p-type contacts. With a protective coating on the top surface, the Si substrate is etched and tungsten is deposited from the backside in order to introduce a higher strain. Figure 4(b) is an image from optical microscope showing a strained PD.

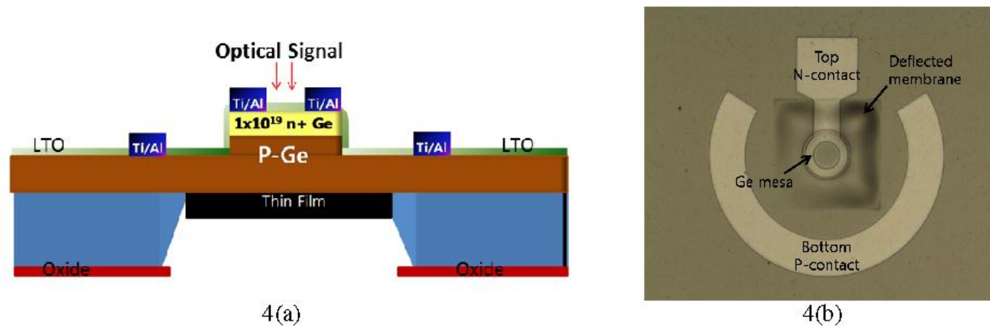

Fig. 4. (a) Schematic diagram of strained Ge PN photodetector (b) Optical image of a strained PD showing a deflected active region

The photocurrent measurement was conducted by shining light from a tunable optical parametric oscillator on the center of the mesa while the device was under 1V bias. Figure 5 shows the normalized photocurrent spectra from three different samples with 0.2%, 0.58%, and 0.76% bi-axial tensile strain. The device with a 0.2% strained active region shows a roll-off of the measured photocurrent below 1.6um due to the direct band gap in Ge. Notably, PDs with both 0.58% and 0.76% bi-axial tensile strain show an excellent responsivity well beyond 1.6um. This effect can be attributed to the direct band gap reduction in Ge resulting in an enhanced absorption for longer wavelengths. Multiple peaks at around 1.55μm and 1.7μm are due to the Fabry-Perot cavity enhancement from the free-standing Ge membrane and the inset shows the calculated enhancement factor in the 1.65μm Ge membrane PD using the transfer matrix method [30]. We are currently investigating electroluminescence from this highly-strained Ge diode in the hopes of improving the efficiency of Ge light emitting diodes (LEDs). A benefit of the circular geometry is that whispering gallery modes should be readily available as we move toward a strained-Ge laser.

#154117 - $15.00 USD Received 7 Sep 2011; revised 12 Oct 2011; accepted 16 Oct 2011; published 5 Dec 2011
(C) 2011 OSA

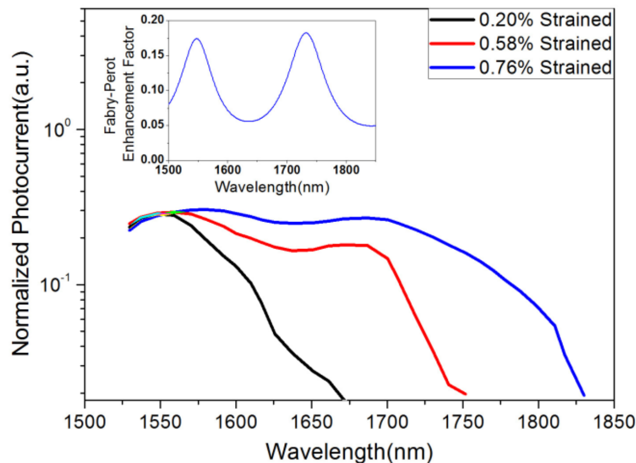

Fig. 5. Normalized photocurrents from strained PDs showing the extended responsivity beyond 1.6um due to the bandgap reduction. Inset shows the calculated Fabry-Perot enhancement factors in a 1.65um Ge membrane, assuming a complex refractive index of n = 4.35, k = 0.01.

5. Conclusion

We have proposed and demonstrated a method to fabricate a thin Ge membrane integrated on a Si substrate and induce a sustainable and large tensile strain by depositing a stressor layer to improve the Ge's optical properties. From room temperature photoluminescence and Raman spectroscopy measurement, larger than 1% biaxial tensile strain is confirmed in highly strained membranes and a direct band gap energy reduction of 100meV is observed. Light emission efficiency from the 1.13% strained membrane was significantly improved compared to the 0.2% strained membrane, as predicted in our simulation for the fraction of electrons in the Γ valley vs. strain. According to our tight-binding calculations, population inversion in 1% strained and heavily doped Ge can be achieved with two orders of magnitude less injection than unstrained and undoped Ge. Moreover, we presented the first device fabrication using highly strained Ge and showed an excellent responsivity well beyond 1.6µm from a 0.76% strained Ge photodetector. We believe that our strain-tunable membrane can ultimately be utilized for high efficiency near-infrared lasers, which are essential to realize on-chip optical interconnects.

Acknowledgments

This work was supported by U.S. Government through APIC (Advanced Photonic Integrated Circuits) corporation and the Connectivity Center of the Focus Center Research Program, a National Science Foundation Graduate Research Fellowship under Grant No. DGE-0645962, a Stanford Graduate Fellowship and a Fonds Québécois de la Recherche sur la Nature et les Technologies Master's Research Scholarship.

(C) 2011 OSA